Spin-dependent negative differential conductance in transport through single-molecule magnets*

Luo Wei(罗 威), Wang Rui-Qiang(王瑞强)†, Hu Liang-Bin(胡梁宾), and Yang Mou(杨 谋)

Laboratory of Quantum Information Technology, ICMP and SPTE, South China Normal University, Guangzhou 510006, *China*

(Received 11 September 2012; revised manuscript received 18 October 2012)

Transport properties are theoretically studied through an anisotropy single-molecule magnet symmetrically connected to two identical ferromagnetic leads. It is found that even though in parallel configuration of leads' magnetizations, the total current still greatly depends on the spin polarization of leads at certain particular bias region, and thus for large polarization a prominent negative differential conductance (NDC) emerges. This originates from the joint effect of single-direction transitions and spin polarization, which removes the symmetry between spin-up and spin-down transitions. The present mechanism of NDC is remarkably different from the previously reported mechanisms. To clarify the physics of the NDC, we further monitored the shot noise spectroscopy and found that the appearance of the NDC is accompanied by the rapid decrease of Fano factor.

Keywords: spintronics, single-molecule magnets, negative differential conductance, shot noise

PACS: 72.25.–b, 75.50.Xx, 73.23.Hk, 72.70.+m **DOI:** 10.1088/1674-1056/22/4/047201

1. Introduction

The electronic transport through single molecule junctions[1,2] has attracted great interest large partly with a goal to develop molecular circuits. With spin as an additional degree of freedom participating in the electronic transport, there molecular spintronics,[3] as an extension of molecular electronics, has emerged recently. The molecular spintronics is of interest for fundamental physics, e.g., it can shed new insight into mechanisms for molecular-scale spin-resolved transport. An ideal playground for study of molecular spintronics is the tunnel junction consisting of single-molecule magnets (SMMs),[4–6] such as Mn_{12} or Fe_8. Especially, research of the electrically-controlling transport through the SMMs has become an active subject.

The structure of SMMs combines the classical properties of magnets with the intrinsic quantum nature. The outstanding features lie in its large spin and remarkable magnetic anisotropies. At low temperatures, the magnetic anisotropy barrier forbids the spin reversal between the degenerated states with opposite spins, forming long-living bistable magnetic states where the spin quantum tunneling happens. Early studies mostly focused on the spin quantum effect of isolated SMMs.[7,8] Very recently, however, considerable effort is devoted to the transport spectra through an individual magnetic molecule. In a single-molecule-transistor geometry, it is demonstrated that the molecule magnetic anisotropy can be preserved and even electrically controllable.[9] In the transport spectra, the signatures of magnetic states and magnetic anisotropy can be identified experimentally.[4,5] Apart from this, various quantum effects in SMM junctions have been observed or predicted. For example, spin-selection rules associated with the magnetic anisotropy can lead to complete suppression of current,[4] spin diode behavior,[10] and pure spin current in thermoelectric effect.[11,12] Applying spin-polarized current, manipulation of spin switching of nanomagnets is possible.[13–17] Under the joint effect of exchange interactions and spin quantum tunneling, Kondo effect arisen from the SMMs was predicted theoretically.[18–20]

In the transport through the SMMs, the appearance of negative differential conductance (NDC) is an interesting phenomena and has been oberved experimentally in N/SMM/N junction (N denotes the normal metal).[4] This NDC was interpreted as the blockade of electronic transport when a sequence of tunnel processes result in a nonequilibrium population of certain excited states that can be depopulated only slowly by violation of the selection rules. For the same system, Timm and Elste[21] suggested that NDC features may appear even in the case of no blocking state, which is simply as a consequence of the difference in the weight of transition rates for the allowed transitions between various molecular states. A typical mechanism for the NDC is Pauli spin blockade, which is in connection with the exchange singlet–triplet splitting and has been studied widely in double quantum dot.[22–24] In contrast to the Pauli spin blockade, the spin blockade in the SMMs is formed under the joint effect of the magnetic anisotropy and spin-flip exchange interactions.[10,25,26] When the magnetic state is saturated at the singly-charged state with minimal or

*Project supported by the Program for New Century Excellent Talents in University of China (Grant No. NCET-10-0090), the National Natural Science Foundation of China (Grant Nos. 10974058, 11174088, and 11274124), and the Natural Science Foundation of Guangdong Province of China (Grant No. S2012010010681).

†Corresponding author. E-mail: rqwanggz@163.com

© 2013 Chinese Physical Society and IOP Publishing Ltd

maximal magnetism, spin-flip electron tunnelings are blockaded due to the spin-selection rules. In an N/SMM/F asymmetric system (F is ferromagnetic metal), Elste and Timm[25] remarked that the NDC can emerge when the gate voltage is tuned from a Coulomb blockade regime to a spin blockade regime. In this process, an applied external field is necessary to remove the degeneracy of the spin multiplets for the low-temperature NDC but it is not necessary for the high-temperature NDC.

In this paper, we investigate the electronic transport through an SMM symmetrically coupled to two ferromagnetic electrodes. Interestingly, it is found that in parallel configuration of leads' magnetizations, there develops a prominent NDC at certain particular bias region for large polarization. The underlying physics originates from the joint effect of single-direction transitions and spin polarization, which removes the symmetry between spin-up and spin-down transitions due to different ejected rates but the same forbidden injections for two spin species. The present mechanism of NDC is remarkably distinguished from previously reported mechanisms. In order to provide more insight into physics of the NDC, we further calculated the corresponding shot noise spectra by employing the full counting statistics (FCS).[27,28] The shot noise[28,29] proves to be a source of useful information about various transport properties hardly accessible from direct measurement of electric current. In SMM system, the noise spectroscopy has been used to identify the fake resonances in current induced by the spin tunneling,[30] and it is sensitive to the Coulomb interaction and the coupling asymmetry to leads.[31,32] In the present discussion, we found that the appearance of the NDC is accompanied by the rapid decrease of Fano factor (the ratio of shot noise to average current). The organization of the rest of this paper is as follows. In Section 2, a theoretical model and the FCS approach are presented. In Section 3, we first discuss the numerical results of polarization-related current and the appearance of NDC for both ferromagnetic and antiferromagnetic exchange couplings. A short summary is presented in the last section.

2. Model and method

We consider a widely adopted SMM Hamiltonian[14,21,25]

$$H_{\rm SMM} = \sum_{\sigma}(\varepsilon_0 - eV_{\rm g})c^{\dagger}_{\sigma}c_{\sigma} + Uc^{\dagger}_{\uparrow}c_{\uparrow}c^{\dagger}_{\downarrow}c_{\downarrow} - D(S_z)^2 - J\boldsymbol{s}\cdot\boldsymbol{S}, \tag{1}$$

consisting of the on-site energy ε_0 of molecular orbit, the Coulomb repulsion energy U between two electrons, the easy-axis magnetic anisotropy energy D, and the exchange energy J between orbit electron spin $\boldsymbol{s} = \sum_{\sigma\sigma'} c^{\dagger}_{\sigma}(\tau_{\sigma\sigma'}/2)c_{\sigma'}$ and SMM local spin $\boldsymbol{S}$. $c^{\dagger}_{\sigma}(c_{\sigma})$ is the creation (annihilation) operator for orbit electrons and $\tau_{\sigma\sigma'}$ is the matrix element of Pauli vector. The gate voltage $V_{\rm g}$ capacitively coupled to the SMM is to tune ε_0. We assume that the Coulomb repulsion energy $U \to \infty$ is far larger than all the relevant energy parameters and so the double occupation is prohibited energetically. The magnetic anisotropy perpendicular to the easy-axis is shown to be smaller than D by several orders in magnitude and so it can be disregarded safely.

Diagonalizing $H_{\rm SMM}$ in Eq. (1) allows one to denote its eigenstates as $|n,m\rangle$ with n being electron number in the molecular orbit and m being the magnetic quantum number of the z-component of the total spin $\boldsymbol{S}_t = \boldsymbol{S} + \boldsymbol{s}$. For $n = 0$, the eigenstates $|0,m\rangle$ are just those of S_z with eigenvalues $\varepsilon_{|0,m\rangle} = -Dm^2$. For $n = 1$, the eigenstates are given by

$$|1,m\rangle^{\pm} = a^{\pm}(m)\,|{\downarrow}\rangle\left|m+\frac{1}{2}\right\rangle + b^{\pm}(m)\,|{\uparrow}\rangle\left|m-\frac{1}{2}\right\rangle, \tag{2}$$

where the adjacent eigenstates of S_z are mixed by the electron spin state $|\sigma\rangle$ due to the spin exchange coupling. The coefficients are given in Ref. [21], reading $a^{\pm}(m) = \mp\zeta_{\pm}/\sqrt{\triangle\varepsilon}$ and $b^{\pm}(m) = J\sqrt{S(S+1)-m^2+1/4}/(4\zeta_{\pm}\sqrt{\triangle\varepsilon})$ with $\zeta_{\pm} = \sqrt{2\triangle\varepsilon \mp (2D-J)m}/2$ where the symmetry $a^{\pm}(-m) = b^{\pm}(m)$ is guaranteed. The corresponding eigenenergies are

$$\varepsilon_{|1,m\rangle^{\pm}} = \varepsilon_0 - eV_{\rm g} + \frac{J}{4} - D\left(m^2+\frac{1}{4}\right) \pm \triangle\varepsilon(m) \tag{3}$$

with $\triangle\varepsilon(m) \equiv [D(D-J)m^2 + (J/4)^2(2S+1)^2]^{1/2}$. For the fully polarized states $\left|1,\pm S \pm \frac{1}{2}\right\rangle$, the upper subscript corresponds to $D > J/2$ and the lower one to $D < J/2$.

The transport properties of electrons are spin-dependent when the SMM is coupled to two ferromagnetic metallic electrodes through the tunneling Hamiltonian

$$H_{\rm T} = \sum_{\alpha k\sigma}(t_{\alpha}a^{\dagger}_{\alpha k\sigma}c_{\sigma} + {\rm H.c.}) \tag{4}$$

with t_{α} being the tunneling amplitude. The electrodes are modeled as noninteracting Fermi gases $H_{\rm el} = \sum_{\alpha k\sigma}\varepsilon_{\alpha k}a^{\dagger}_{\alpha k\sigma}a_{\alpha k\sigma}$, where $a^{\dagger}_{\alpha k\sigma}$ $(a_{\alpha k\sigma})$ creates (annihilates) an electron with momentum k and spin σ in electrode $\alpha = {\rm L,R}$. It is assumed that the electronic transport is dominated by the sequential tunneling. To find out the average current as well as the shot noise at the same time, we employ the FCS approach.[27,28] Starting with the Liouville–von Neumann equation under the Born and Markov approximations, we obtain a set of master equations[33] in terms of the number-resolved reduced density matrix $\rho^{(n)}(t)$, which is applicable in the case of weak SMM-electrode coupling. The probability $P_i(t)$ of finding the molecule in the state $|i\rangle = |n,m\rangle$ is $P_i(t) = \sum_n P_i^{(n)}(t)$, which involves the sum over n electrons having been transferred during a time interval t. The number-resolved probability $P_i^{(n)}(t)$ is found to satisfy

$$\frac{{\rm d}P_i^{(n)}}{{\rm d}t} = \sum_{j\sigma}[(W^{R,\sigma-}_{j\to i} + W^{R,\sigma+}_{j\to i})P_j^{(n)} + W^{L,\sigma-}_{j\to i}P_j^{(n+1)}$$

$$+W_{j\to i}^{L,\sigma+}P_j^{(n-1)}]-\sum_{\alpha j\sigma}(W_{i\to j}^{\alpha,\sigma+}+W_{i\to j}^{\alpha,\sigma-})P_i^{(n)}. \quad (5)$$

Here, $W_{i\to j}^{\alpha,\sigma+}=\Gamma_{\alpha\sigma}f_\alpha^+(\varepsilon_j-\varepsilon_i)\left|\langle j|c_\sigma^\dagger|i\rangle\right|^2$ stands for the transition rate from electrode α to the SMM and $W_{i\to j}^{\alpha,\sigma-}=\Gamma_{\alpha\sigma}f_\alpha^-(\varepsilon_i-\varepsilon_f)\left|\langle i|c_\sigma^\dagger|j\rangle\right|^2$ is the opposite process with the Fermi distribution function $f_\alpha^+(x)=1/[1+\mathrm{e}^{(x-\mu_\alpha)/k_BT}]$ and $f_\alpha^-(x)=1-f_\alpha^+(x)$. $\left|\langle j|c_\sigma^\dagger|i\rangle\right|^2$ in the transition rates constitutes the basic selection rules for transitions between molecular states, i.e., the transition is allowed only when the charge state of the SMM is changed by 1 and $\Delta m=\pm1/2$. We assume that two leads are in the thermal equilibrium with temperature T and the nonequilibrium transport is driven by a chemical potential $\mu_{L(R)}=\pm eV_b/2$ exerted by an applied bias voltage V_b. $\Gamma_{\alpha\sigma}=2\pi\rho_{\alpha\sigma}|t_\alpha|^2$ characterizes the level-width function with $\rho_{\alpha\sigma}$ as the density of states at the Fermi level of magnetic electrode α. Define a spin polarization of the ferromagnetic electrodes as $\xi=(\rho_\uparrow-\rho_\downarrow)/(\rho_\uparrow+\rho_\downarrow)$ and then the linewidth functions can be expressed as $\Gamma_{L\uparrow(\downarrow)}=\Gamma_{L0}(1\pm\xi)$, and $\Gamma_{R\uparrow(\downarrow)}=\Gamma_{R0}(1\pm\xi)$ for the parallel magnetic alignment while $\Gamma_{R\uparrow(\downarrow)}=\Gamma_{R0}(1\mp\xi)$ for the antiparallel one.

If a counting field χ is introduced to count the number n of electrons emitted from the left lead, it is easy from Eq. (5) to find the quality $S_j(\chi,t)=\sum_n P_j^{(n)}(t)\,\mathrm{e}^{\mathrm{i}n\chi}$, which is determined by

$$\frac{\mathrm{d}S_i(\chi,t)}{\mathrm{d}t}=L_{ij}^\chi S_j, \quad (6)$$

where L^χ is a χ-resolved matrix, whose elements are $L_{ij}^\chi=\mathrm{e}^{-\mathrm{i}\chi}W_{j\to i}^{L,\sigma-}+\mathrm{e}^{\mathrm{i}\chi}W_{j\to i}^{L,\sigma+}+W_{j\to i}^{R,\sigma-}+W_{j\to i}^{R,\sigma+}$ for the nondiagonal components $i\neq j$ and $L_{ii}^\chi=-\sum_{k\neq i}(W_{i\to k}^{L,\sigma-}+W_{i\to k}^{L,\sigma+}+W_{i\to k}^{R,\sigma-}+W_{i\to k}^{R,\sigma+})$ for the diagonal components $i=j$. According to Eq. (6), we can define a cumulant generating function[27,34] $F(\chi)=\lambda_0(\chi)t$, which is determined by the eigenvalue $\lambda_0(\chi)$ of the matrix L^χ if the condition $\lambda_0(\chi)|_{\chi\to0}\to0$ is satisfied. Thus, all the cumulants of the current can be obtained by performing derivatives with respect to the counting field, $C_k=(-\mathrm{i}\partial_\chi)^kF(\chi)|_{\chi=0}$. The transport characteristics are directly related to the cumulants, e.g., average current is given by $I=eC_1/t$ and zero-frequency shot noise by $S=2e^2C_2/t$.

3. Results and discussion

In this section, we perform the numerical results of electronic transport through the SMM. For the convenience of analysis, we calculate a simple SMM with $S=1$, which is enough to capture the essential physics. We also limit to the symmetric coupling $\Gamma_{L0}=\Gamma_{R0}=\Gamma_0$ of the SMM to two identical leads, and fix parameters $\varepsilon_0-eV_g=0.1$ and $T=0.002$ throughout.

3.1. Current–voltage characteristics with NDC

In Fig. 1(a), we plot the current–voltage curves for the SMM with different spin polarizations ξ in parallel alignment of magnetization of leads. Unlike the conventional single-level dot, the SMM exhibits more complex transport characteristics in I–V. First, due to the anisotropy and the spin exchange coupling, the single-orbit level of the SMM is split into $2m+1$ sub-levels [see Fig. 1(b)], which yields more steps in the current curve. Interestingly, in the bias region of $0.35<eV_b<0.45$ the current plateau is ξ-dependent. With increasing ξ, the plateau value is lifted higher. During this process, a dip of current develops gradually in the vicinity of bias threshold $eV_b=0.43$ for a new channel opening, accompanied by a visible NDC. It is emphasized that the present developed ξ-dependent NDC appears for the parallel alignment of magnetizations, which is significantly distinguished from the previous mechanisms in SMM system,[10,25] where the system structure is asymmetric, i.e., consists of a ferromagnetic lead and a normal metal lead. To clarify the underlying physics, we will in the following analyze the occupation probability of each state since the magnitude of current is determined by occupation probabilities and rates of transition.

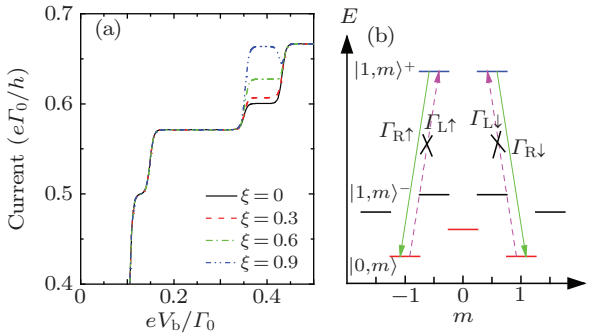


Fig. 1. (color online) (a) Current I as a function of bias voltage eV_b in parallel alignment of magnetizations for different polarizations ξ with $J=0.1$ and $D=0.04$. (b) Schematic view for the magnetic levels of SMM with magnetic quantum number m.

First, we discuss the unpolarized case with $\xi=0$ and plot the probability of each state in Fig. 2(a) as a function of bias voltage. With the increase of bias, the multiplet channels open one by one: Each transition corresponds to a current step in Fig. 1(a). In particular, the first transitions between $|0,\pm1\rangle$ and $|1,\pm3/2\rangle$ contribute to the biggest step of current, and then other transitions $|0,\pm1\rangle\rightleftharpoons|1,\pm1/2\rangle^-$, $|0,0\rangle\rightleftharpoons|1,\pm1/2\rangle^+$, and $|0,\pm1\rangle\rightleftharpoons|1,\pm1/2\rangle^+$ are in turn responsible for other current steps. This order is arranged according to the level difference between states in Fig. 1(b). Especially, one can notice a unique bias region of $\varepsilon_{|1,\pm1/2\rangle^+}-\varepsilon_{|0,0\rangle}<eV_b/2<\varepsilon_{|1,\pm1/2\rangle^+}-\varepsilon_{|0,\pm1\rangle}$ (namely, $0.35<eV_b<0.45$ for chosen parameters), where the opening of transport channels $|0,0\rangle\rightleftharpoons\left|1,\pm\frac{1}{2}\right\rangle^+$ increases the probability $P_{\left|1,\pm\frac{1}{2}\right\rangle^+}$ only a little but enhances $P_{|0,\pm1\rangle}$ and $P_{\left|1,\pm\frac{3}{2}\right\rangle}$ significantly, different from the

case of the other channel openings. The reason is that $P_{|1,\pm\frac{1}{2}\rangle^+}$ are depleted to the sates $|0,\pm1\rangle$ through the single-direction transitions, i.e., the process $|1,\pm\frac{1}{2}\rangle^+ \to |0,\pm1\rangle$ is allowed but the opposite one is energetically prohibited, as shown in Fig. 1(b). When the bias is sufficient large ($eV_b > 0.45$), all of the states participate in the transport and have the same occupation probability, which is equivalent to the usual dot. In addition, one can also notice that the degenerated doublets $|n,m\rangle$ and $|n,-m\rangle$ always have the same probability due to the unpolarized electron transports.

Next, we discuss the case of ferromagnetic leads aligned in parallel and plot the relevant occupation probability in Fig. 2(b). Compared to the case of $\xi = 0$, a distinct characteristic for finite ξ is that, in the particular bias region of $0.35 < eV_b < 0.45$ the probabilities of degenerate doublets $|n,m\rangle$ and $|n,-m\rangle$ ($m \neq 0$) are lifted and their original weights are redistributed between them. As a result, there arises a magnetic accumulation $\langle m\rangle = \sum_i m_i P_i$ in the molecular subsystem, as shown in the inset of Fig. 2(b), where $\langle m\rangle$ increases with ξ and vanishes for $\xi = 0$. The crucial point to this is the existence of available single-direction transitions $|1,\pm\frac{1}{2}\rangle^+ \to |0,\pm1\rangle$ where the nonzero probabilities of $|1,\pm\frac{1}{2}\rangle^+$ are maintained through the processes $|0,0\rangle \to |1,\pm\frac{1}{2}\rangle^+$. We can understand the magnetic accumulation from the electron subsystem. One should notice the following facts. In the large bias region, the electrons tunnel only from left to right lead and the opposite process can be negligible. The transitions $|0,m\rangle \to |1,m+\frac{1}{2}\rangle^\pm$ and $|0,m\rangle \to |1,m-\frac{1}{2}\rangle^\pm$ are companied, respectively, by the injection of spin-up electrons with rate $\Gamma_{L\uparrow}$ and spin-down electrons with rate $\Gamma_{L\downarrow}$ from left lead to the SMM. The reversal transitions are related to the ejection from the SMM to right lead with rate $\Gamma_{R\uparrow}$ for spin-up electrons and with rate $\Gamma_{R\downarrow}$ for spin-down electrons. When the bidirection transitions $|0,m\rangle \rightleftharpoons |1,m\pm\frac{1}{2}\rangle^\pm$ are available, for each spin species the tunneling-in electrons are always equal to the tunneling-out electrons due to $\Gamma_{L\sigma} = \Gamma_{R\sigma}$ for chosen parameters. However, this situation is changed for the single-direction transitions $|1,\frac{1}{2}\rangle^+ \to |0,1\rangle$ and $|1,-\frac{1}{2}\rangle^+ \to |0,-1\rangle$, which are opened at the same time due to the same energy difference. The opening of these two single-direction transitions has twofold meanings: i) The electron injection is prohibited energetically, and ii) the allowed electron ejection is in different rates for two spins, i.e., the former is in $\Gamma_{R\downarrow}$ and the latter is in $\Gamma_{R\uparrow}$. As a result, the accumulation $\langle m\rangle$ appears, which is equal to the difference between oriented-up spin and oriented-down spin. This is quite different from the early studies,[10,25,35–37] where the magnetic accumulation (or spin accumulation) is generated by preparing the electron injection and the electron ejection in different rates $\Gamma_{L\sigma} \neq \Gamma_{R\sigma}$, i.e., the molecule is coupled to two ferromagnetic leads in antiparallel alignment or coupled to a ferromagnetic lead and a normal lead. In contrast, out of the bias window $0.35 < eV_b < 0.45$, all states are involved in bidirectional transitions $|0,m\rangle \rightleftharpoons |1,m\pm\frac{1}{2}\rangle^\pm$, where the equal rates of injection and ejection ($\Gamma_{L\sigma} = \Gamma_{R\sigma}$) for each pair of bidirectional transitions make all the probabilities ξ-independent.

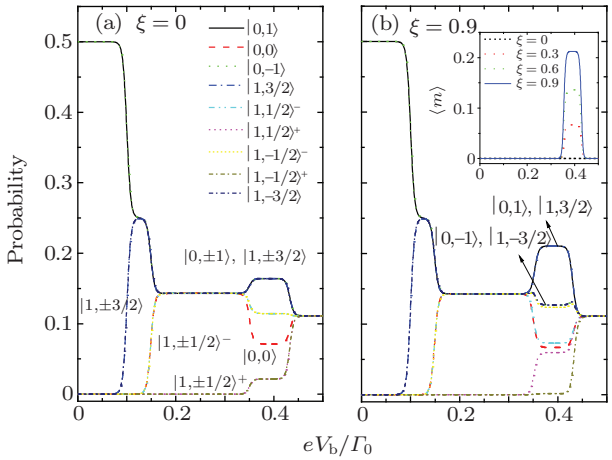


Fig. 2. (color online) Occupation probabilities of states as a function of bias voltage eV_b (a) for unpolarized leads $\xi = 0$ and (b) for high-polarized leads $\xi = 0.9$. Inset is the magnetic accumulation $\langle m\rangle$ for different ξ. The other chosen parameters are the same as those in Fig. 1.

Having known the ξ-dependent occupation probability, we now can interpret easily the ξ-dependence of current and the formation of NDC in Fig. 1(a). The current is contributed by transitions in pairs, e.g., $I^{\uparrow}_{|0,1\rangle\to|1,3/2\rangle} \propto |b^\pm(3/2)|^2(1+\xi)P_{|0,1\rangle}$ and $I^{\downarrow}_{|0,-1\rangle\to|1,-3/2\rangle} \propto |a^\pm(-3/2)|^2(1-\xi)P_{|0,-1\rangle}$ and so $I^{\uparrow}_{|0,1\rangle\to|1,3/2\rangle} + I^{\downarrow}_{|0,-1\rangle\to|1,-3/2\rangle} \propto 2P_0 + \xi\,|b^\pm(3/2)|^2(P_{|0,1\rangle} - P_{|0,-1\rangle})$ where $P_0 = (P_{|0,1\rangle} + P_{|0,-1\rangle})/2$ and $a^\pm(-3/2) = b^\pm(3/2)$. Out of the bias window $0.35 < eV_b < 0.45$, all probabilities $P_{|n,m\rangle}$ are equal and so the polarization ξ can be always canceled in each pair. This is a typical property in quantum dot for parallel configuration of magnetization. Within the bias window, however, it is not a case. For example, $I^{\uparrow}_{|0,1\rangle\to|1,3/2\rangle} + I^{\downarrow}_{|0,-1\rangle\to|1,-3/2\rangle}$ increases with ξ since the retribution of probabilities results in $P_{|0,1\rangle} > P_{|0,-1\rangle}$ and almost keeps P_0 a constant. Among all transitions, the transitions of $|0,\pm1\rangle \to |1,\pm3/2\rangle$ play a dominant role due to their largest probabilities and transition rates and thereby the total current for finite ξ is larger than the total current for $\xi = 0$. In the vicinity of the threshold bias associated with transitions $|0,\pm1\rangle \to |1,\pm\frac{1}{2}\rangle^+$, there exists two competitive mechanisms: The opening of the new channels $|0,\pm1\rangle \to |1,\pm\frac{1}{2}\rangle^+$ increases the current but meanwhile decreases the probability $P_{|0,1\rangle}$ down to the average value among all states which in turn shrinks the current. As a consequence, in this crossover region a current dip develops, accompanied by the appearance of an NDC. The width of the dip is determined by temperature T. As the bias voltage is increased up to the energy difference $eV_b/2 = \varepsilon_{|1,\pm1/2\rangle^+} - \varepsilon_{|0,\pm1\rangle}$, the current recovers the situation of ξ-independence.

The variation of the NDC with the magnetic parameters is illustrated in Fig. 3, where the current as a function of bias voltage is shown for different exchange couplings J [Fig. 3(a)] and for different anisotropy barriers D [Fig. 3(b)] with spin polarization set to be $\xi = 0.9$. It is obvious that the NDC dip can keep stable lineshape for larger J or smaller D. Exchange interaction J describes the ability of the SMM to exchange spin with the electron while anisotropy D describes the energy barrier to overcome in spin reversal of the SMM. For smaller J or larger D, it is difficult to redistribute the occupation probabilities between doublets $|n,\pm m\rangle$, unfavorable for the formation of the NDC mechanism mentioned above. Therefore, in order to observe the NDC experimentally, we could adjust J and D, leting the former increase or the latter decrease. In addition, it is noticed that large J shifts the NDC dip to the high bias with unchanged width of ξ-dependent current plateau while large D widens the plateau with unchanged central position of the current plateau. This can be understood as follows. Since the first step in Figs. 3(a) and 3(b) corresponds to the level difference $2(\varepsilon_{|1,\pm1/2\rangle^+} - \varepsilon_{|0,0\rangle})$ and the second to $2(\varepsilon_{|1,\pm1/2\rangle^+} - \varepsilon_{|0,\pm1\rangle})$, both of which increase with J. The plateau width is determined by their energy difference, i.e., $2(\varepsilon_{|1,\pm1/2\rangle^+} - \varepsilon_{|0,\pm1\rangle}) - 2(\varepsilon_{|1,\pm1/2\rangle^+} - \varepsilon_{|0,0\rangle}) = 2(\varepsilon_{|0,0\rangle} - \varepsilon_{|0,\pm1\rangle})$, which is obviously independent of J but is sensitive to D.

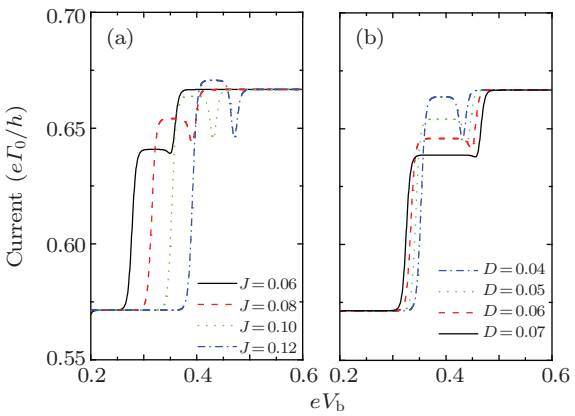


Fig. 3. (color online) Current I versus bias voltage eV_b for (a) different J with $D = 0.04$, and (b) different D with $J = 0.1$. Magnetic leads are in parallel configuration with $\xi = 0.9$.

In the above discussions, we consider the situation of ferromagnetic ($J > 0$) interaction between a conducting electron and SMM's spin. In a realistic case, the exchange interaction can be either ferromagnetic or antiferromagnetic ($J < 0$), depending on the specific type of the SMM. In Fig. 4(a), the I–V curves are plotted for different ξ for $J < 0$. Similar to the ferromagnetic coupling in Fig. 1(a), the antiferromagnetic coupling also can lead to the ξ-dependent current at a bias window $\varepsilon_{|1,\pm1/2\rangle^+} - \varepsilon_{|0,0\rangle} < eV_b/2 < \varepsilon_{|1,\pm1/2\rangle^+} - \varepsilon_{|0,\pm1\rangle}$ (namely, $0.23 < eV_b < 0.46$ for chosen parameters) and a prominent NDC at $2(\varepsilon_{|1,\pm3/2\rangle^+} - \varepsilon_{|0,\pm1\rangle}) \simeq 0.3$ for strong ξ. The underlying physics stems from the same spin-dependent single-direction transitions $\left|1,\pm\frac{1}{2}\right\rangle^+ \to |0,\pm1\rangle$, which give rise to the separation between probabilities of degenerate states $|n,m\rangle$ and $|n,-m\rangle$ ($m \neq 0$), as shown in Fig. 4(b). Here, the probabilities contributed by the states with $m < 0$ are dominant and so a negative magnetic accumulation arises due to the antiferromagnetic exchange interaction, in contrast to the case of $J > 0$. Compared with Fig. 1(a), although the ξ-dependent current in Fig. 4(a) exists in a broad bias range, ξ-enhanced part is compressed to a narrow region $0.25 < eV_b < 0.30$ and the position of the NDC is shifted to $eV_b = 0.3$. The essential cause is that, for $J < 0$ the energy of states $|1,\pm3/2\rangle$ becomes higher than the energy of states $\left|1,\pm\frac{1}{2}\right\rangle^-$ and the opening of the channel with energy $\varepsilon_{|1,\pm3/2\rangle} - \varepsilon_{|0,\pm1\rangle}$ is in between energies $\varepsilon_{|1,\pm1/2\rangle^+} - \varepsilon_{|0,0\rangle}$ and $\varepsilon_{|1,\pm1/2\rangle^+} - \varepsilon_{|0,\pm1\rangle}$. This significantly reduces $P_{|0,\pm1\rangle}$ and then suppresses the current to the value even smaller than the unpolarized case in the region $0.30 < eV_b < 0.46$. When we tune the parameters $|J|$ and D, the curves have the similar variation as that in Fig. 3. In addition, one can notice that at $eV_b = 2(\varepsilon_{|0,\pm1\rangle} - \varepsilon_{|1,\pm1/2\rangle^-}) \simeq 0.15$, there exists another NDC. Unlike the above case, this NDC is independent of ξ due to ξ-independent probability distribution. This NDC was reported previously in the unpolarized transport through the SMM.[21] We can interpret the ξ-independent NDC with the similar physics mechanism. When new channels $|0,0\rangle \to |1,\pm1/2\rangle^-$ are opened, the current at the first plateau

$$I = \frac{e}{2} W^{\mathrm{L},+}_{|0,\pm1\rangle \to |1,\pm1/2\rangle^-}$$

is reduced to the second plateau

$$I = \frac{2e}{5}(W^{\mathrm{L},+}_{|0,\pm1\rangle \to |1,\pm1/2\rangle^-} + W^{\mathrm{L},+}_{|0,0\rangle \to |1,\pm1/2\rangle^-}).$$

The latter is smaller than the former due to

$$W^{\mathrm{L},+}_{|0,0\rangle \to |1,\pm1/2\rangle^-} < \frac{1}{4} W^{\mathrm{L},+}_{|0,\pm1\rangle \to |1,\pm1/2\rangle^-}$$

following from the m-related coefficients $a^-(m)$ and $b^-(m)$.

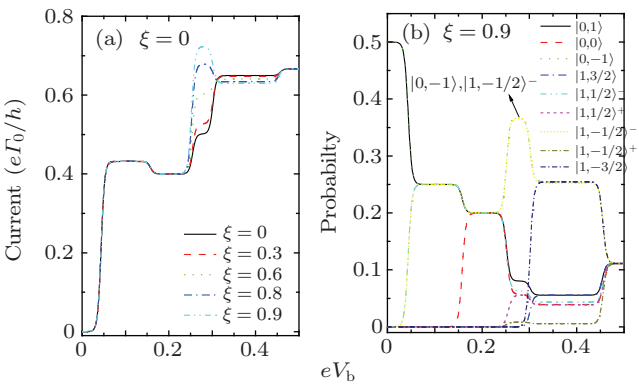


Fig. 4. (color online) (a) Current I for different ξ and (b) probabilities of states with fixed $\xi = 0.9$ as a function of eV_b. Magnetic leads are in parallel configuration with $J = -0.1$ and $D = 0.04$.

3.2. Shot noise spectra for NDC

To understand the NDC clearly, we further monitor shot noise spectra (second cumulant), which is frequently applied to reveal the dynamical correlation between electron channels, originating from the electron fluctuation in nonequilibrium transports. Fano factor F, defined as the rate of shot noise to current, $F = S/2eI = C_2/C_1$, is employed to measure the deviation from the stochastic Poissonian statistics ($F = 1$). We display the Fano factor F as a function of bias voltage in Fig. 5(b) for ferromagnetic coupling $J > 0$ and in Fig. 5(d) for antiferromagnetic coupling $J < 0$. The corresponding currents are plotted in Figs. 5(a) and 5(c) for reference. Compared the current and the corresponding Fano factor, a common pronounced characteristic for both $J > 0$ and $J < 0$ is that the appearance of NDC in the current is companied with a rapid shrink of Fano factor: A Fano factor step for $J > 0$ while a Fano factor dip for $J < 0$. This situation becomes prominent with the increase in polarization ξ. If $\xi = 0$, the Fano factor is of sub-Poissonian type ($F < 1$). For a moderate ξ, e.g., $\xi = 0.3$ for $J < 0$, we can observe the transition of super-Poisson ($F > 1$) to sub-Poisson ($F < 1$) as the applied bias is tuned.

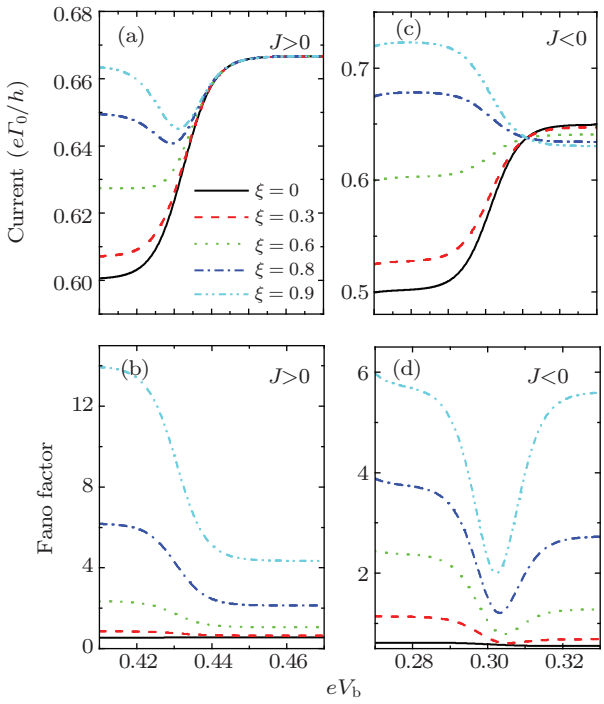


Fig. 5. (color online) Currents I (a) and (c), and Fano factors F (b) and (d) as a function of eV_b for different ξ. Panels (a) and (b) are for ferromagnetic coupling $J = 0.1$ with $D = 0.04$, and panels (c) and (d) are for antiferromagnetic coupling $J = -0.1$ in parallel magnetic configuration.

Obviously, the underlying dynamical mechanism stems from the spin-dependent electron transports. There are involved in two types of dynamical mechanism. On the right of the NDC region, $F > 1$ is attributed to the dynamical spin blockade as proposed in Refs. [34], [38], and [39]. In the case of spin polarization with the parallel alignment, although the total current is ξ-independent but the spin-dependent currents $I_\uparrow$ and $I_\downarrow$ are unequal. There exists a fast ($I_\uparrow$) transport channel and a slow ($I_\downarrow$) transport channel. For the spin-up electrons, it is a longer time waiting during the spin-down electrons tunneling out of the SMM due to time $1/\Gamma_\downarrow > 1/\Gamma_\uparrow$. However, once this slow process is finished, a large numbers of spin-up electrons will consecutive flow through the dot within a shorter time interval until a spin-down electron tunnels in again, giving rise to bunching effect of the spin-up electrons. As a consequence, the increase of ξ makes F exhibit a sub-to-super-Poissonian statistics crossover. On the left of the NDC region, besides the above spin dynamical blockade, the magnetic accumulation, as a super-Poissonian dynamical mechanism, contributes additionally to F. This mechanism was studied in strongly asymmetric magnetic single-electron transistors.[40] One can recall that the accumulation $\langle m \rangle$ for $J > 0$ is positive while that for $J < 0$ is negative. For $J > 0$, the positive accumulation acts on the electrons via spin blockade effect, which makes spin-up channel (dominated by $|0,1\rangle \rightleftharpoons |1,3/2\rangle$) more faster and the spin-down channel (dominated by $|0,-1\rangle \rightleftharpoons |1,-3/2\rangle$) slower. This strengthens spin fluctuation between two spin channels and presents an F step when the bias goes through the NDC region. In contrast, for $J < 0$, the negative accumulation favors the spin-down electron transport but hampers the spin-up electron transport. As a result, the spin-down tunneling instead becomes the fast channel and the spin-up tunneling becomes the slow channel. The competition between them leads to a super-Poisson noise. When the bias approaches the vicinity of dip of F, coexistence of two mechanisms leads to the comparable magnitude in two channel currents. This destroys the competition of two spin channels and greatly suppresses the spin fluctuation close to the Poissonian behavior.

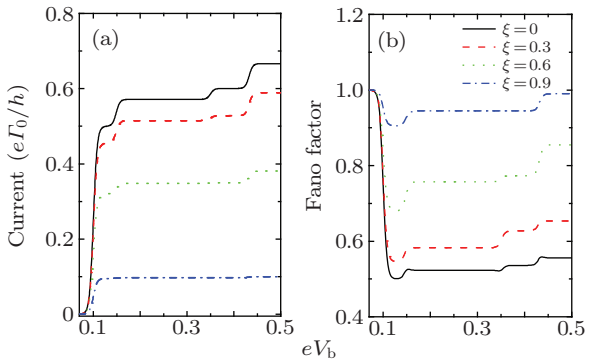


Fig. 6. (color online) (a) Current I and (b) Fano factors F as a function of eV_b for different ξ. Magnetic leads are in antiparallel configuration with $J = 0.1$ and $D = 0.04$.

Finally, we wish to address the situation of the antiparallel magnetization of ferromagnetic leads. The I–V curves for this configuration are plotted in Fig. 6(a). Here, one cannot observe the NDC. Besides the complicate multi-step, the main feature is the suppressed current for finite ξ. This attributes

to the spin mismatch when an electron transfers from the spin majority (minority) in one lead to the spin minority (majority) in the other lead. In Fig. 6(b) our calculations also show that, the shot noise is always of sub-Poissonian type though it is enhanced with increase of ξ. Compared to the usual quantum dot, the SMM in the antiparallel magnetic configuration does not exhibit more characteristics except for some steps in lineshape.

4. Summary

Electronic transport through an anisotropy SMM coupled to two ferromagnetic leads is investigated by employing the full numerical statistics approach. We focus on a symmetry structure with two identical magnetic leads aligned in parallel magnetization. Interestingly, a polarization-dependent current is found at certain particular bias region, which is accompanied by the appearance of a prominent NDC for strong leads' polarization. The present NDC distinguishes remarkably from the early-proposed mechanism based on either asymmetrical magnetic structure or magnetic field broken spin-rotation symmetry. The underlying physics is the joint effect of the single-direction transitions and spin-polarized transport. This joint effect breaks the symmetry between spin-up and spin-down transitions due to different spin-dependent ejected rates for two spin species. We present the detailed interpretation by analyzing the occupation probability and the magnetic accumulation in the SMM. We also present the variation of NDC with magnetic parameters for the cases of ferromagnetic and antiferromagnetic exchange couplings. To understand the dynamical mechanism of the NDC, we further study the shot noise spectroscopy and find that the NDC is manifested by the decrease of Fano factor. It is expected that our results can be tested in the SMM system as in recent experiments.[4–6]

References

[1] Zimbovskaya N A and Pederson M R 2011 *Phys. Rep.* **509** 1
[2] Andergassen S, Meden V, Schoeller H, Splettstoesser J and Wegewijs M R 2010 *Nanotechnology* **21** 272001
[3] Bogani L and Wernsdorfer W 2008 *Nat. Mater.* **7** 179
[4] Heersche H B, de Groot Z, Folk J A, van der Zant H S J, Romeike C, Wegewijs M R, Zobbi L, Barreca D, Tondello E and Cornia A 2006 *Phys. Rev. Lett.* **96** 206801
[5] Jo M H, Grose J E, Baheti K, Deshmukh M M, Sokol J J, Rumberger E M, Hendrickson D N, Long J R, Park H K and Ralph D C 2006 *Nano Lett.* **6** 2014
[6] Henderson J J, Ramsey C M, del Barco E, Mishra A and Christou G 2007 *J. Appl. Phys.* **101** 09E102
[7] Wernsdorfer W and Sessoli R 1999 *Science* **284** 133
[8] Wernsdorfer W, Sessoli R, Caneschi A, Gatteschi D and Cornia A 2000 *Europhys. Lett.* **50** 552
[9] Zyazin A S, van den Berg J W G, Osorio E A, van der Zant H S J, Konstantinidis N P, Leijnse M, Wegewijs M R, May F, Hofstetter W, Danieli C and Cornia A 2010 *Nano Lett.* **10** 3307
[10] Misiorny M, Weymann I and Barnaś J 2010 *Europhys. Lett.* **89** 18003
[11] Wang R Q, Sheng L, Shen R, Wang B G and Xing D Y 2010 *Phys. Rev. Lett.* **105** 057202
[12] Zhang Z Z, Jiang L, Wang R Q, Wang B G and Xing D Y 2010 *Appl. Phys. Lett.* **97** 242101
[13] Misiorny M and Barnaś J 2007 *Phys. Rev. B* **75** 134425
[14] Misiorny M and Barnaś J 2007 *Phys. Rev. B* **76** 054448
[15] Delgado F, Palacios J J and Fernández-Rossier J 2010 *Phys. Rev. Lett.* **104** 026601
[16] Lu H Z, Zhou B and Shen S Q 2009 *Phys. Rev. B* **79** 174419
[17] Zhang Z Z, Shen R, Sheng L, Wang R Q, Wang B G and Xing D Y 2011 *Chin. Phys. B* **20** 047504
[18] Romeike C, Wegewijs M R, Hofstetter W and Schoeller H 2006 *Phys. Rev. Lett.* **96** 196601
[19] Romeike C, Wegewijs M R, Hofstetter W and Schoeller H 2006 *Phys. Rev. Lett.* **97** 206601
[20] Wang R Q and Xing D Y 2009 *Phys. Rev. B* **79** 193406
[21] Timm C and Elste F 2006 *Phys. Rev. B* **73** 235304
[22] Liu H W, Fujisawa T, Hayashi T and Hirayama Y 2005 *Phys. Rev. B* **72** 161305
[23] Rudner M S and Levitov L S 2007 *Phys. Rev. Lett.* **99** 036602
[24] Coish W A and Qassemi F 2011 *Phys. Rev. B* **84** 245407
[25] Elste F and Timm C 2006 *Phys. Rev. B* **73** 235305
[26] Wang R Q, Shen R, Zhu S L, Wang B G and Xing D Y 2012 *Phys. Rev. B* **85** 165432
[27] Bagrets D A and Nazarov Y V 2003 *Phys. Rev. B* **67** 085316
[28] Wang S K, Jiao H, Li F, Li X Q and Yan Y J 2007 *Phys. Rev. B* **76** 125416
[29] An X T, Li Y X and Liu J J 2007 *Acta Phys. Sin.* **56** 4105 (in Chinese)
[30] Romeike C, Wegewijs M R and Schoeller H 2006 *Phys. Rev. Lett.* **96** 196805
[31] Xue H B, Nie Y H, Li Z J and Liang J Q 2011 *Phys. Lett. A* **375** 716
[32] Xue H B, Nie Y H, Li Z J and Liang J Q 2010 *J. Appl. Phys.* **108** 033707
[33] Ouyang S H, Lam C H and You J Q 2010 *Chin. Phys. B* **19** 050519
[34] Cottet A, Belzig W and Bruder C 2004 *Phys. Rev. Lett.* **92** 206801
[35] Wang R Q, Zhou Y Q, Wang B G and Xing D Y 2007 *Phys. Rev. B* **75** 045318
[36] Souza F M, Egues J C and Jauho A P 2007 *Phys. Rev. B* **75** 165303
[37] Hu L B, Gao J and Shen S Q 2004 *Phys. Rev. B* **70** 235323
[38] Lindebaum S, Urban D and König J 2009 *Phys. Rev. B* **79** 245303
[39] Wang R Q, Sheng L, Hu L B, Wang B G and Xing D Y 2011 *Phys. Rev. B* **84** 115304
[40] Bulka B R, Martinek J, Michalek G and Barnaś J 1999 *Phys. Rev. B* **60** 12246